Journal of Macromolecular Science, Part A
Publication details, including instructions for authors and subscription information:
http://www.informaworld.com/smpp/title~content=t713597274

Electrosynthesis of a Net-like Microstructured Poly(*p*-aminophenol) Film Possessing Electrochemical Properties in a Wide pH Range

Chuanxiang Chen[ab]; Cheng Sun[a]; Yuhua Gao[b]
[a] State Key Laboratory of Pollution Control and Resource Reuse, School of the Environment, Nanjing University, Nanjing, P.R. China [b] Department of Chemistry, School of Materials Science and Engineering, Jiangsu University of Science and Technology, Zhenjiang, P.R. China

To cite this Article Chen, Chuanxiang , Sun, Cheng and Gao, Yuhua(2008) 'Electrosynthesis of a Net-like Microstructured Poly(*p*-aminophenol) Film Possessing Electrochemical Properties in a Wide pH Range', Journal of Macromolecular Science, Part A, 45: 12, 972 — 979
To link to this Article: DOI: 10.1080/10601320802453690
URL: http://dx.doi.org/10.1080/10601320802453690

Journal of Macromolecular Science®, Part A: Pure and Applied Chemistry (2008) **45**, 972–979

ISSN: 1060-1325 print / 1520-5738 online
DOI: 10.1080/10601320802453690

Taylor & Francis
Taylor & Francis Group

Electrosynthesis of a Net-like Microstructured Poly(*p*-aminophenol) Film Possessing Electrochemical Properties in a Wide pH Range

CHUANXIANG CHEN[1,2], CHENG SUN[1,*] and YUHUA GAO[2]

[1]*State Key Laboratory of Pollution Control and Resource Reuse, School of the Environment, Nanjing University, Nanjing 210093, P.R. China*
[2]*Department of Chemistry, School of Materials Science and Engineering, Jiangsu University of Science and Technology, Zhenjiang 212003, P.R. China*

Received April 2008 and accepted May 2008

Electrochemical polymerization of *p*-aminophenol in aqueous sulfuric acid solution has been carried out at a platinum foil using repeated potential cycles at the range of −0.20 to 0.95 V (vs. SCE). The resulting polymer has good electrochemical activity and a fast charge transfer characteristic in the solutions of 0.5 mol dm^{-3} Na_2SO_4 with pH ≤ 9.0. Based on the spectroscopic measurements, a possible chemical structure of the resulting polymer was proposed. IR and XPS spectra indicate that SO_4^{2-} ions are contained in the resulting polymer. The scanning electron microscopy (SEM) micrograph proves that the net-like microstructure of the poly(*p*-aminophenol) film, which is a macroporous network composed of interwoven and coalescing fiber diameters of 100–500 nm and pore diameters of 500 nm–3 μm, can be prepared using the electrochemical method.

Keywords: *p*-Aminophenol, poly(*p*-aminophenol), electrochemical polymerization, electrochemical properties, XPS

1. Introduction

Among conducting polymers, polyaniline has been widely studied due to its ease of synthesis, exciting electrochemical activity, excellent electrochromic property, high conductivity and good environmental stability. These properties make it suitable for several potential applications in sensors, biosensors, rechargeable batteries, electrochromic devices and others. In addition, a number of researchers have also investigated polyaniline microstructures (1). In particular, the template-free preparation of polyaniline microstructures is expected to open new applications for polyaniline (2,3). However, polyaniline generally has little electrochemical property at pH > 4. This limits its practical applications such as biosensors. One way to improve the electrochemical property is by polymerizing aniline derivatives with hydroxyl (4), alkoxy (5), carboxyl (6), sulfo (7), alkyl (8) or aryl (9) group substitutions.

Indeed, the electrochemical oxidation of *o*-aminophenol, a hydroxy derivative of aniline, was carried out at different electrode materials in aqueous acidic solutions to form an electroactive polymer. The resulting polymer had a significantly higher electrochemical activity than polyaniline, and was applied to fabricate sensors or biosensors (10–16). Taking into account the fact that *p*-aminophenol (*p*-APh), like *o*-aminophenol, is also a hydroxyl aniline derivative, one could grow a polymer from *p*-APh. Unfortunately, although many authors have investigated the electrooxidation of *p*-APh and found that the oxidation product was *p*-quinomeimine, which suffered hydrolysis to *p*-benzoquinone, no film formation was observed or mentioned (17–20). However, Taj et al. reported that electropolymerization of *p*-APh on a platinum electrode yielded an electroactive polymer in non-aqueous medium. They obtained a poly(*p*-aminophenol) (PPAP) film with electrochemical properties at pH ≤ 4 (21). Eddy et al. (22), Ekinci et al. (23) and Han et al. (24) reported the elecrosynthesis of the PPAP in aqueous media to produce biosensors. Madurro and coworkers (25–27) investigated the electrochemical modifications of graphite and gold substrates with PPAP in aqueous acidic solutions. According to these authors, there are no studies of the PPAP film with electrochemical activity at pH > 4 although they were able to

*Address correspondence to: Cheng Sun, State Key Laboratory of Pollution Control and Resource Reuse, School of the Environment, Nanjing University, Nanjing 210093, P.R. China. Tel./Fax: +86-25-83593239. E-mail: envidean@nju.edu.cn (C Sun); cxchenyz@yahoo.com.cn (CX Chen)

obtain a polymer film upon the electrooxidation of *p*-APh in both aqueous and non-aqueous media.

It was generally accepted that the properties of polyaniline can be improved by changing experimental conditions (28) and that electropolymerization from acidic aqueous media was preferable for formation of an electroactive polymer (29). This suggests that electrochemical properties of PPAP may be affected by the electropolymerization conditions, such as the electrode materials, aqueous and non-aqueous electrolytes, controlled potential and current density, etc. Here we report an electropolymerization of *p*-APh on a platinum anode in an aqueous sulfuric acid solution to yield a polymer with a good electrochemical activity at pH $\leq$ 9.0, which is much better than that of the one synthesized by previous literature methods. Scanning electron microscopy (SEM), UV-vis spectrum, infrared spectrum (IR) and X-ray photoelectron spectroscopy (XPS) of the PPAP film obtained here are also examined.

2. Experimental

p-APh (99%, HPLC grade) was obtained from Riedel–deHaën (Germany) and used without further purification. H_2SO_4, Na_2SO_4 and NaOH were of analytical reagent grade and purchased from Shanghai Chemical Regent Corporation (China). Doubly distilled water was used to prepare solutions

The electrochemical synthesis and voltammetric experiments were performed using a traditional three-electrode with two platinum foil electrodes and a saturated calomel reference electrode (SCE, all potentials are given against this reference). The area of the platinum foil was $4 \times 4\,mm^2$. A CHI 650A electrochemical workstation (CH Instrument Co., USA) connected to a computer was used in all electrochemical experiments at room temperature.

The electrochemical polymerization of *p*-APh was carried out by means of the cyclic voltammetry in a solution consisting of 0.2 mol dm^{-3} *p*-APh, and 0.5 mol dm^{-3} H_2SO_4. The scan rate was 100 mV s^{-1}. The scan potential range was controlled from -0.20 to 0.95 V.

Cyclic voltammetry of the polymer film was performed using a CHI 650A electrochemical workstation in a solution of 0.5 mol dm^{-3} H_2SO_4 first, and then in solutions of 0.5 mol dm^{-3} Na_2SO_4 with various pH values. The scan rate was set at 50 mV s^{-1}, except for the effect of the scan rate on the shape of $i-E$ curves.

Before recording a cyclic voltammogram, the polymer film was pre-treated for five cycles in the following testing solutions of sodium sulfate. This aim is to establish pre-equilibrium of pH between the film and the test solution. The pH value of sodium sulfate solution was set in a pH range of 1.0 to 9.0. The pH values of solutions were determined using a model PHS-25C pH meter (Shanghai Kangyi Co., China) by mixing water and Na_2SO_4 and then adjusting the pH value with a solution of NaOH or H_2SO_4.

UV–Vis absorptive spectra of *p*-APh in 0.5 mol dm^{-3} Na_2SO_4 and dried PPAP powder were performed on a Model U-3010 UV-Vis spectrophotometer (Hitachi, Japan).

The surface structure and chemical composition of the polymer film were analyzed by *ex site* attenuated total reflectance infrared (ATR-IR) and X-ray photoelectronic spectroscopy (XPS). The infrared spectra of the dried *p*-APh powder and the PPAP film were obtained using a NEXUS 870 Fourier transform infrared spectrometer (Nicolet, USA) in conjunction with horizontal ATR accessory with germanium crystal. The resolution of the spectra was 4 cm^{-1}, and scans were repeated 32 times. X-ray photoelectron spectroscopy (XPS) analyses were carried using an ESCALab 250 spectrometer (Thermo VG Scientific, USA) with Al Kα at 1486.6 eV. All binding energies were referenced to the C 1s peak at 284.8 eV of the surface adventitious carbon.

Scanning electron microscopy (SEM) image of the PPAP film was measured on a JSM-6480 SEM instrument (JEOL, Japan) operating at an acceleration voltage of 20 kV. The sample for the electron microscope was sputter-coated with platinum.

3. Results and discussion

3.1. *Electropolymerization of p-Aph*

Figure 1 shows the cyclic voltammograms of film growth during the electrolysis of *p*-APh. There is a well-defined anodic peak at about 0.67 V and a shoulder at about 0.77 V for the first cycle (curve 1). The two anodic peaks also appear on the second cycle (curve 2) but their peak potentials are both shifted to higher values and their peak currents decease somewhat. Furthermore, the shoulder on curve 1 becomes a pronounced peak on curve 2, while the anodic peak at more negative potentials becomes a shoulder. The anodic peak situated at more negative potentials could be ascribed to the fact that the adsorbed *p*-APh undergoes a first $1e^-/1H^+$ reaction to the radical; the additional one at more positive potentials could be attributed to the fact that the radical absorbed on the electrode surface suffers a $1e^-/1H^+$ reaction to *p*-quinoneimine (QI), which disperse towards the bulk solution and is subsequently hydrolyzed into *p*-benzoquinone (Q) (30,31). A 1,4-addition (Michael addition) of *p*-APh to Q or QI occurs rapidly to yield amine-substituted quinones or amine-substituted hydroquinones for the first cycle (20–32), which can be oxidized and reacts with *p*-APh via a 1,4-addition for the second cycle. For the third cycle, the anodic shoulder almost disappears. A single anodic peak appears at more than 0.67 V and it shifts slightly towards positive potentials from the forth cycle afterwards. This is due to the fact that the polymer film grows with time.

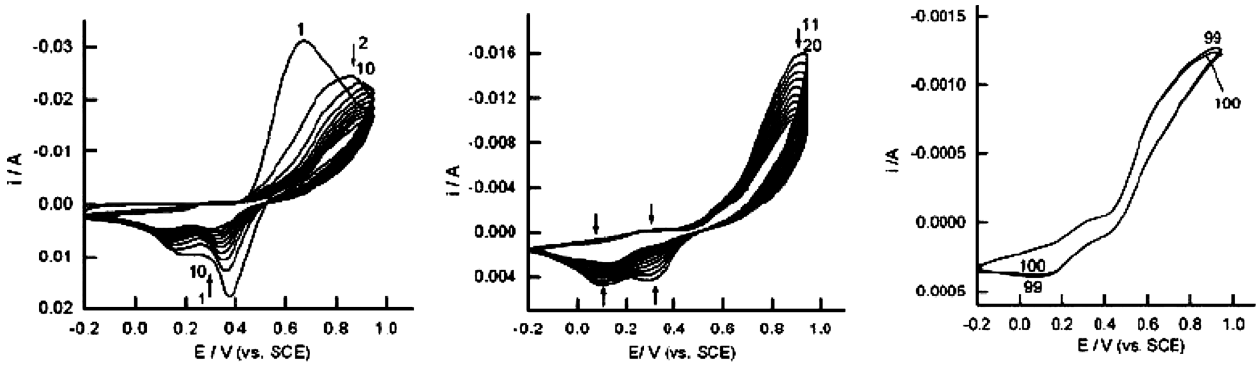

Fig. 1. Cyclic voltammograms of polymerization of *p*-APh. Solution composition: 0.5 mol dm^{-3} H_2SO_4 and 0.2 mol dm^{-3} *p*-APh. Scan rate: 100 mV s^{-1}. The number of curves in the plot corresponds to the number of cycles.

Besides that, two cathodic peaks occur at about 0.17 and 0.37 V on curve 1, a third anodic peak at about 0.29 V and two cathodic peaks appear at about 0.14 and 0.36 V for the second cycle (curve 2). The third anodic peak around 0.29 V and the cathodic peak around 0.14 V is attributed to the reduction/reoxidation of the polymer film itself (27), but also to the overlapping of Q. The cathodic peak at about 0.36 V is assigned to the reduction of QI. The two cathodic peak currents decrease slowly and their peak potential shift more negatively a little with increasing scan cycles from the first to fifteen cycle (Fig. 1A and 1B). This is due both Q and QI concentrations decreasing slowly during the electrolysis, taking into account that they both take part in a polymer film formation.

However, the cathodic peak at higher potentials disappears slowly and the two cathodic peaks change into a peak with increasing scan cycles from the sixteen to 100th cycle (Figs. 1B and 1C). This is also due to the film thickness of the resulting polymer deposited onto the working electrode is increasing during the electrolysis. This result is similar to the electrochemical polymerization behavior presented in Reference (28).

After electrodeposition, electrodes were thoroughly rinsed using a solution of 0.5 mol dm^{-3} H_2SO_4 to remove unreacted *p*-APh and then using doubly distilled water before use in the following characterization experiments. This purification is enough to evaluate the electrochemical properties and structure of the resulting polymer.

3.2. *Cyclic voltammograms* CV*s of the polymer*

3.2.1. *Effect of pH value on the cyclic voltammograms*

Figure 2 shows the cyclic voltammograms of a PPAP film in 0.5 mol dm^{-3} Na_2SO_4 solutions at various pH values at 50 mV s^{-1}.

As seen in Figure 2, the PPAP exhibits two separate redox couples, respectively. Both redox couples shift towards more negative potentials with increasing the pH values from 1.0 to 9.0. This reveals that each of the two redox processes of the polymer at more negative potentials is related to proton concentration of the solution, i.e., protons in the polymer enter into the solution for the oxidation process, and vice versa for the reduction process. We also observed that each cathodic peak current (i_{pc}) was kept approximately equal to its corresponding anodic peak current (i_{pa}), and that the separation of the peak potentials, ΔE_p, increases with increasing pH value. This was due to that the electrochemical behavior of the polymer, at the

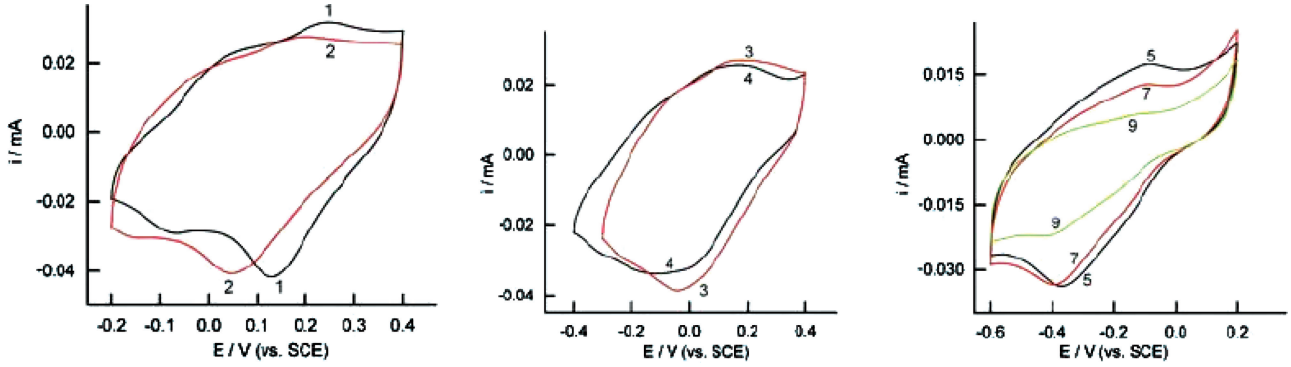

Fig. 2. Effect of pH value on the cyclic voltammograms of PPAP in 0.5 mol dm^{-3} Na_2SO_4 solutions. Scan rate: 50 mV s^{-1}. The number of curves in the plot corresponds to the pH values.

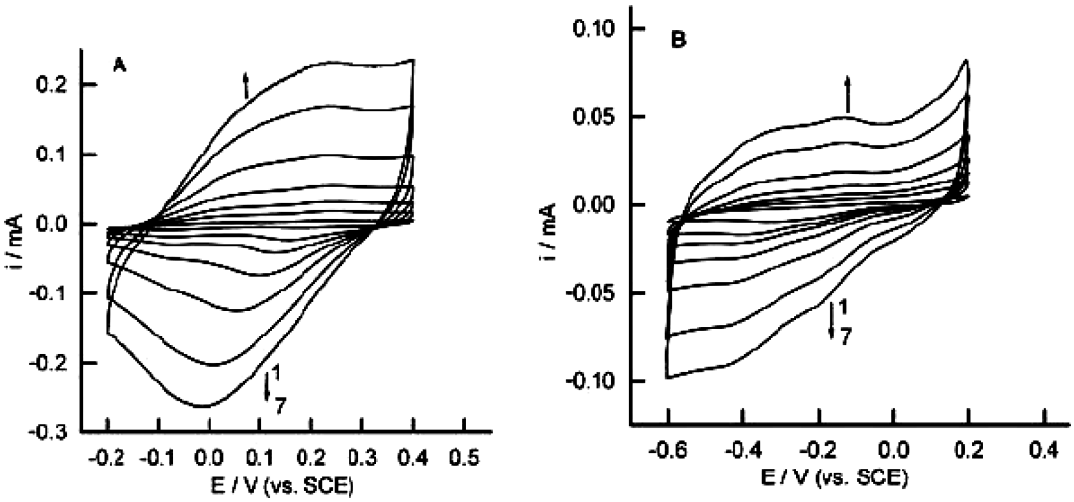

Fig. 3. Effect of potential scan rate on the cyclic voltammograms of PPAP in a solution of 0.5 mol dm^{-3} H_2SO_4 (A) and in a solution 0.5 mol dm^{-3} Na_2SO_4 with pH 9.0 (B). Scan rates: 5, 25, 50, 100, 200, 400, 600 mV s^{-1}.

platinum electrode, corresponds to two reversible signals in the above pH range.

In general, there are two redox couples of polyaniline at pH < 4.0 (33). One occurs around 0.10 V, which is almost independent of pH value and is caused by doping and dedoping of anions (34); the other occurs at about 0.74 V (at pH 1.0), which peak potentials shift toward more negative values with increasing pH values (35), but i_{pc} is normally approximately twice that of i_{pa}. Thus, the electrochemical properties of polyaniline are different from those of the PPAP obtained here. This is mainly attributed to a —OH functional side group in the PPAP, which can be oxidized to quinone and quinone can be reduced reversibly. As for the PPAP in an aqueous solution, the redox couple situated at more negative potentials could be ascribed to the redox reaction of a —OH side group in the PPAP, i.e., the electron transfer is coupled with proton exchange between the polymer and the solution. The additional redox wave at more positive potentials could be attributed to the redox reaction of the polymer main chain, i.e., the redox process is accompanied with doping and dedoping of anions. This phenomenon is similar to what is observed in the case of a polymer with other redox-active side groups. The above results mean the PPAP is a redox polymer.

In addition, it should be noted that the cyclic voltammogram of PPAP in 0.5 mol dm^{-3} H_2SO_4 solution (vide infra) is similar to the one in the solution of 0.5 mol dm^{-3} Na_2SO_4 with pH 1.0 at 50 mV s^{-1}.

The above results indicate that the PPAP has a good electrochemical activity in a wide pH range in the solution of sodium sulfate with pH ≤ 9.0. This is mostly attributed to the hydroxyl functional groups in the polymer chain.

3.2.2. *Effect of the scan rate on the cyclic voltammograms*

Figure 3A shows that the cyclic voltammograms of PPAP in 0.5 mol dm^{-3} H_2SO_4 solution at various scan rates. It is observed that each peak current increases with increasing scan rate, and that each peak potential, except for the cathodic peak at higher potentials, with an increase in the scan rates from 5 to 600 mV s^{-1} shift hardly. As seen in Fig. 3A, there are still two pairs of redox peaks at 600 mV s^{-1}. This indicates that the electrochemical reaction is still controlled by mass transfer at such a high scan rate. On the basis of the relationship between the scan rate υ and each anodic (cathodic) peak current, the peak currents varied linearly with $\upsilon^{1/2}$. This again identifies that the electrode reaction of PPAP is controlled by mass transfer and the PPAP film still has a good ability of the charge transfer in an aqueous acid solution.

Figure 3B shows that the cyclic voltammograms in a solution of 0.5 mol dm^{-3} Na_2SO_4 with pH 9.0 at various scan rates. In the plot, there are also two redox couples, which peak potentials are almost not shifted with increasing scan rates. There are also two pronounced redox couples at 600 mV s^{-1} on curve 7. Thus, it could be concluded that the electrode reaction of PPAP is controlled by mass transfer and PPAP has an ability of the charge transfer at pH 9.0.

3.3. *UV-Vis spectra*

Curves 1 and 2 in Figure 4 display the UV-Vis spectra of *p*-APh in 0.5 mol dm^{-3} H_2SO_4 solution and dried PPAP powder in air, respectively. As seen in Figure 4, three peaks at 195, 230 and 300 nm appear on curve 1, and they also occur on curve 2. However, curve 2 shows a new broad but well-defined peak at 473 nm, which would be attributed to the π-π^* conjugation chain of PPAP. This result is in agreement with the color of the polymer film, which is golden. The above difference between curves 1 and 2 reveals that the electrooxidation of *p*-APh can form a polymer film on the electrode surface.

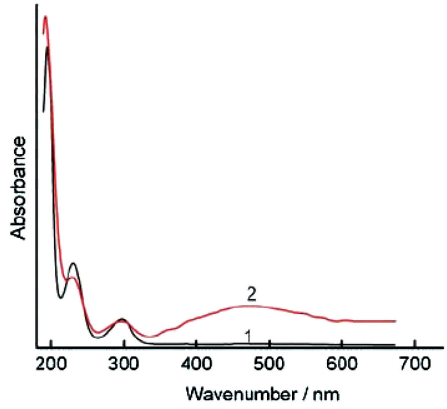

Fig. 4. UV-Visible spectra for *p*-APh (1) and PPAP (2).

3.4. *IR spectra*

Curves 1 and 2 in Figure 5 show the IR spectra of *p*-APh and PPAP, respectively. Both spectra in Figure 5 are the same as those presented in Reference (28). The IR spectrum of PPAP obtained here is different from that of the polymer electrosynthesized on a platinum electrode in a non-aqueous medium (21) or on a gold substrate in an aqueous sulfuric acid solution (27), in which a absorption band at 3274 cm^{-1} in IR spectrum of the monomer disappeared (21), or two absorption peaks at 1511 and 1474 cm^{-1} in the monomer spectrum almost disappeared (27). However, the band around 3274 cm^{-1} appears but shifts to 3217 cm^{-1} in curve 2, and the two strong peaks at 1511 and 1474 cm^{-1} also occur. Furthermore, a pronounced shoulder at 1497 cm^{-1} is accompanied by the peak around 1511 cm^{-1} in curve 2, while the peak at 1474 cm^{-1} shifts to1442 cm^{-1} and its the intensity is somewhat weaker in curve 2 than in curve 1. In addition, the peaks at 2815, 2682, 2591, 2496, 1150, 1010, 968 and 919 cm^{-1} almost disappear in curve 2. The above differences between curves 1and 2 reveal that the polymer was formed after electrolysis.

The peak in the monomer at 3340 cm^{-1}, attributed to N–H stretching vibrations (36), almost disappear in curve 2, whilst the peak at 3274 cm^{-1}, assigned as O–H stretching vibrations (36), is replaced by a new broad intense band around 3217 cm^{-1} for the PPAP. This indicates the presence of the free –OH groups and the absence of the free $-NH_2$ groups in the polymer. As shown in curve 1, the three peaks at 3179, 3031 (36) and 2815 cm^{-1} (21) are attributable to stretching vibrations of C–H in phenyl ring, the peak at 2919 cm^{-1} is assigned to stretching vibrations of C=C in phenyl ring (21), and the three peaks at 2682, 2591 and 2496 cm^{-1} are attributed to the formation of hydrogen bonds among the monomers (37). However, beside the new band at 3217 cm^{-1}, three weak peaks at 3179, 3031 and 2919 cm^{-1} also appear in curve 2, respectively. This means that C–H bonds in phenyl ring changed and that hydrogen bonds were destroyed after polymerization.

Four peaks of the monomer at 1614, 1509,1474 and 1387 cm^{-1}, attributed to C–C stretching vibrations (36), appear in curve 2 but shift to 1610 (shoulder), 1512 1445 and 1360 cm^{-1}, respectively. However, a new shoulder peak at 1496 cm^{-1}, assigned to stretching vibrations of N–H in second amine –NH– groups, occurs in spectrum 2, indicating that the transformation of a primary to a second amine and that the polymerizing chains grow through the amino groups. Furthermore, a strong absorption peak appears at 1563 cm^{-1}, which is assigned as the formation of a C=N structure (38). In addition, a C=O stretching vibration peak appears at 1635 cm^{-1} in spectrum 2, revealing that some of the –OH side groups in the polymer have be oxidized.

The six C–H in-plane bending vibration peaks of *p*-APh at 1255, 1236, 1168, 1150, 1119 and 1093 cm^{-1} (36) almost disappear in the polymer spectrum, but four new peaks at 1245, 1188, 1167 and 1102 cm^{-1} occur in the latter. The peak of the polymer at 1245 cm^{-1} is attributed to C–N stretching vibrations (38) or phenyl ring torsion vibrations (20). The new three peaks at 1188, 1167 and 1102 cm^{-1} are all assigned to HSO_4^- and SO_4^{2-} ions (20). This means that HSO_4^- and SO_4^{2-} ions have been doped into the polymer film during the polymerization process. Besides that, a peak of the monomer at 1216 cm^{-1}, attributed to a mixture of C–O and O–H vibrations (36), also occurs but becomes a shoulder at 1219 cm^{-1} in curve 2, which again indicates the presence of free –OH groups in the polymer. However, one C–C–C trigonal bending vibration peak at 1010 cm^{-1}(36), three C–H out-of-plane bending vibration peaks at 968, 919 and 897 cm^{-1} and one C–C stretching vibration peak at 845 cm^{-1} almost disappear in the polymer spectrum. This reveals that H or other groups in phenyl ring could be replaced after the electrolysis.

In addition, three peaks at 749, 705 and 684 cm^{-1} appear in the monomer spectrum. They are attributed to C–OH stretching, $-NH_2$ wagging and O–H out-of-plane bending vibrations, respectively (36). The two peaks at 749 and 684 cm^{-1} appear but shift to 755 and 695 cm^{-1} in curve 2, meanwhile a new O–H out-of-plane bending vibration peak occurs at 725 cm^{-1}. Besides that, a C–OH stretching vibration peak of the monomer at 825 cm^{-1} appears and is not shifted in curve 2. Moreover, a new C–OH stretching vibration peak at 800 cm^{-1} also occurs in the polymer spectrum. It should be noted that the peak at 705 cm^{-1} disappears in curve 2, indicating that $-NH_2$ group has changed into –NH– group after the polymerization. The above results are in agreement with the evidence of the presence of the free –OH group and the absence of the free $-NH_2$ group in the polymer obtained from the IR spectra near 3200–3400 cm^{-1}.

Taking into account the fact that the C–OH stretching vibration peaks of *o*-, *m*- and *p*-aminophenols occur at 800, 822 and 825 cm^{-1} (36) and that the peaks at 825 and 800 cm^{-1} appear in curve 2, we believe that –OH should be attached to the *ortho*-position and *para*-position of amino in a phenyl ring. This is also in agreement with

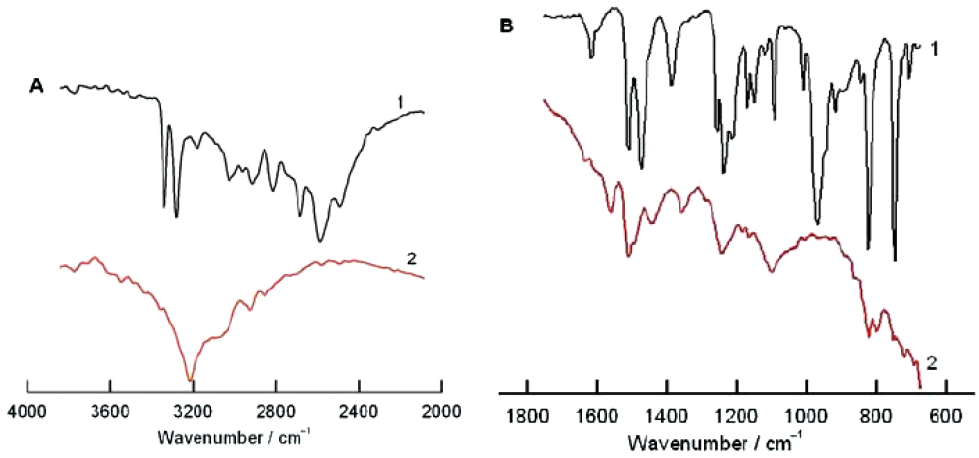

Fig. 5. IR spectra in the wavenumber region of 2000–4000 cm^{-1} (A) and 2000–700 cm^{-1} (B) for *p*-APh (1) and PPAP (2).

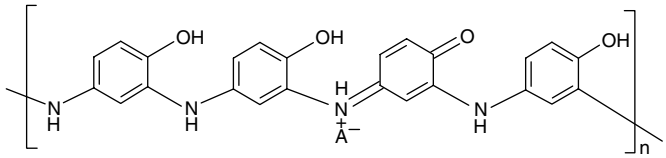

Sch. 1. Possible chemical structure of the PPAP.

the discussion in Section 3.1, where we suggest that the polymer could be electrosynthesized from *p*-APh by an oxidation-Michael addition.

Based on the above discussion, the possible chemical structure of the PPAP is shown in Scheme 1, where A^- is an anion doping the polymer film. It seems that the chemical structure of the PPAP obtained here is somewhat different from that electrosynthesized on platinum in a non-aqueous medium (21), but is somewhat similar to that formed though enzymatic catalysis (38). Taj et al. suggested that both $-OH$ and $-NH_2$ groups of *p*-APh took part in formation of the polymer main chain, *i.e.* there were phenyl-*N*-phenyl and phenyl-*O*-phenyl bonds in the polymer chain (21).

3.5. *XPS of the PPAP*

The chemical state of atoms on the PPAP surface was analyzed by XPS analysis (Fig. 6). As seen in Figure 6A, there are C, N, O and S atoms in the polymer. The first three atoms (C, N and O) are expected since they came from the *p*-APh monomer. Sulfur atom came from H_2SO_4 which was used as the supporting electrolyte in this work. This means that oxygen atom is also attributed to doped SO_4^{2-} and HSO_4^- ions in the polymer (see Section 3.4). In addition, oxygen atom may also be attributed to the oxygen and water adsorbed in the polymer.

The XPS spectrum of C 1s is presented in Figure 6B. The C 1s core level spectrum involved five peaks at 291.3, 288.8, 287.1, 286.2 and 284.8 eV for the polymer. The weak and broad peak at 291.3 eV is a C1s shake-up satellite peak due to a π-π^* transition in aromatic molecules (39). The other four peaks indicate that there are at least four different carbon atoms with different electronic states. It is clear that the C 1s spectrum of the PPAP obtained here is different from that of normal polyaniline since the latter is split into three peaks in the binding energy range between 284 and 289 eV (40). As shown in Figure 6B, the peak at 288.8 eV is referred to C=O bonds, since the carbon atom is attached to an electro-negative oxygen atom *via* a double bond, i.e. the chemical environment of the C atom is different from those of other C atoms. The O atom plays a role in decreasing the shielding of the positive nuclear charges of C 1s by outer electrons. Thus, the effective attractive force of the nucleus with regard to the core electrons of C 1s is increased, *i.e.* its binding energy should be higher than those of other carbon atoms in the polymer. In addition, according to the results obtained by Kang et al. (40) and Su et al. (41) and the above effect of attached electro-negative atoms, the peak at 287.1 eV is assigned to $C{=}N^+$ or $C{-}N^+$ bonds, the peak at 286.2 eV is attributed to t C–OH, C–N or C=N bonds, and the most intense peak at 284.8 eV is referred to C–C or C–H bonds.

The XPS spectrum of O 1s is presented in Figure 6C. The O 1s core level spectrum involved three peaks at 533.5, 532.1 and 531.0 eV for the polymer. The first peak at 533.5 eV, also the most intense one, may come from C–O–H groups (42) and adsorbed H_2O (41), the second one at 532.0 eV should be originating from C=O groups (42), and the third one at 531.1 eV could come from SO_4^{2-} and HSO_4^- ions (43).

There is a single peak in the S 2p and N 1s core level XPS spectra (not shown here). Although the relative content of the sulfur atom is only 0.2%, the small amount of sulfur atom indicates the sulfate and bisulfate ions were doped into the polymer. The XPS N 1s peak with bending energy of 399.9 eV is attibuted to the imine (–N=) and amine

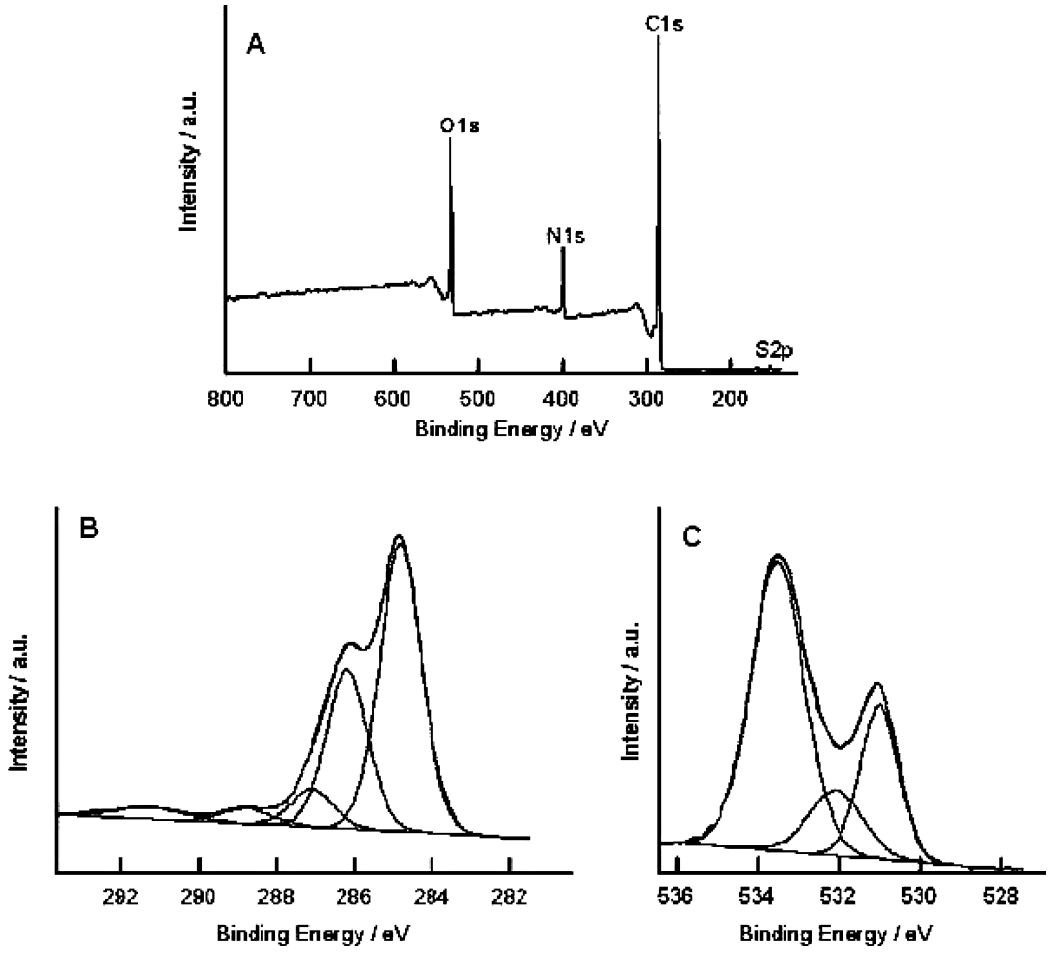

Fig. 6. XPS survey scan spectrum of the PPAP film deposited on Pt. (A) full survey spectrum, (B) C 1s scan spectrum and (C) O 1s scan spectrum.

(–NH–) nitrogens (44). The above XPS results reveal that SO_4^{2-} and HSO_4^- anions could be doped in the resulting polymer and coupled with the protonated nitrogen of PPAP.

3.6. *SEM micrograph of the PPAP*

SEM image of the electrodeposited PPAP film suggests a formation of a highly porous network deposit (Fig.7). The morphology of the polymer is similar to that presented in Reference (28). Both a film-like deposit and a net-like deposit with macropores are observed. The porous network is composed of interwoven and coalescing fiber diameters of 100–500 nm and pore diameters of 500 nm–3 μm.

The above net-like topography formation mechanism may be related to the pattern of "bubbles" visible within some pores, similar to the cause of electrodeposited cellulose films (45). The initially formed continuous PPAP film may undergo a mechanical change at the electrode during reconstitution of polymer fibrils and a net-like microstructure formation may be favorable. Once the pores have opened, the subsequent growth of the deposit strengthens the net-like topography. Thus, it can be obtained a polymer film with a porous network microstructure.

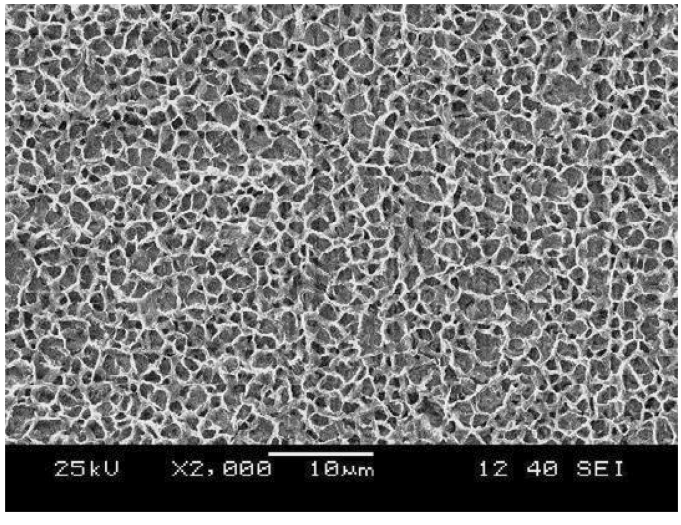

Fig. 7. SEM micrograph of the PPAP film.

4. Conclusions

An electroactive polymer has been formed on platinum during continuous potential cycling in a sulfuric acid solution containing *p*-APh and has a good electrochemical activity and a fast charge transfer characteristic in aqueous solutions with pH $\leq$ 9.0. The effect of the scan rate on the cyclic voltammograms of the PPAP in aqueous solutions reveals that the polymer in both solutions has an electrochemical reversibility and a charge transfer characteristic and the electrode reaction rate of the polymer is controlled by mass diffusion. The SEM morphology shows that the PPAP film has a macroporous network surface microstructure. Based on the UV–vis and IR spectra, a possible chemical structure of the resulting polymer is proposed here, *i.e*. the polymer chain was formed *via* the phenyl-*N*-phenyl bonds. IR spectra and XPS data also prove that both HSO_4^- and SO_4^{2-} are co-dopants of the resulting polymer. However, the electropolymerization mechanism and chemical and surface structures of the resulting polymer are rather complicated, thus a further study on them is required. Its applications are also to be investigated in detail.

Acknowledgments

This work was supported by the National Natural Science Foundation of China (no. 20704020), the National High Technology Research and Development Program ("863" Program) of China (no. 2006AA06Z411) and the Social Development Foundation of Zhenjiang (no. SH2006076). Thanks are given to Professor Jianxin Wu (Center of Physics and Chemistry, University of Science and Technology of China) for his help in the XPS determination.

References

1. Huang, J.X., Virji, S., Weiller, B.H. and Kaner, R.B. (2003) *J. Am. Chem. Soc.,* 125(2), 314–315.
2. Zhong, W., Wang, Y., Yan, Y., Sun, Y., Deng, J. and Yang, W. (2007) *J. Phys. Chem. B*, 111(15), 3918–3926.
3. Zhang, J., Shan, D. and Mu, S.L. (2007) *Polymer*, 48(5), 1269–1275.
4. Harun, M.K., Lyon, S.B. and Marsh, J. (2005) *Prog. Org. Coat.,* 52(3), 246–252.
5. Koval'chuk, E.P., Stratan, N.V., Reshetnyak, O.V., Blazejowski, J. and Whittingham, M.S. (2001) *Solid State Ionics*, 141–142, 217–224.
6. Benyoucef, A., Huerta, F., Vázquez, J.L. and Morallon, E. (2005) *European Polym. J*., 41(4), 843–852.
7. Kitani, A., Satoguchi, K., Tang, H.Q., Ito, S. and Sasaki, K. (1995) *Synth. Met*., 69(1–3), 129–130.
8. Wei, Y., Hariharan, R. and Patel, A. (1990) *Macromalecules*, 23(3), 758–764.
9. Guay, J. and Lê, H.D. (1989) *J. Electroanal. Chem*., 274(1–2), 135–142.
10. Kunimura, S., Ohsaka, T. and Oyama, N. (1988) *Macromalecules*, 21(4), 894–900.
11. Salavagione, H.J., Arias, J., Garcés, P., Morallón, E., Barbero, C. and Vázquez, J. L. (2004) *J. Electroanal. Chem*., 565(2), 375–383.
12. Shah, A.A. and Holze, R. (2006) *J. Electroanal. Chem.,* 597(2), 95–102.
13. Zhang, Y.Y., Wang, M.L., Liu, M.L., Yang, Q., Xie, Q.J. and Yao, S.Z. (2007) *Chin. J. Anal. Chem*., 35(5), 685–690.
14. Tao, W., Pan, D., Liu, Y., Nie L. and Yao, S., (2005) *Anal. Biochem*., 338(2), 332–340.
15. Nassef, H.M., Radi, A.E. and O'Sullivan, C.K. (2006) *Electrochem. Commun*., 8(11), 1719–1725.
16. Li, J. and Lin, X.Q. (2007) *Biosens. Bioelectron*., 22(12), 2898–2905.
17. Heras, A.M., Avila, J.L., Ruiz, J.J. and García-Blanco, F. (1984) *Electrochim. Acta*, 29(4), 541–545.
18. Schwarz, J., Oelßner, W., Kaden, H., Schumer, F. and Hennig, H. (2003) *Electrochim. Acta*, 48(17), 2479–2486.
19. Salvagione, H.J., Arias, J., Garcés, P., Marallón, E., Barbero, C. and Vázquez, J.L. (2004) *J. Electroanal. Chem*., 565(2), 375–383.
20. Song, Y.Z, (2007) *Spectrochim. Acta, Part A*, 67(3–4), 611-618.
21. Taj, S., Ahmed, M.F. and Sankarapapavinasam, S. (1992) *J. Electroanal. Chem*., 338(1-2), 347–352.
22. Eddy, S., Warriner, K., Christie, I., Ashworth, D., Purkiss, C. and Vadgama, P. (1995) *Biosens. Bioelectron*., 10(9–10), 831–839.
23. Ekinci, E., Karagözler, A.A. and Karagözler, A.E. (1996) *Electroanalysis*, 8(6), 571–574.
24. Han, J.H., Taylor, J. D., Kim, D.S., Kim, Y.S., Kim, Y.T. Cha, G.S. and Nam, H. (2007) *Sens. Actuators B*, 123(1), 384–390
25. Vieira, S.N., Ferreira, L.F., Franco, D.L., Afonso, A.S., Gonçalves, R.A., Brito-Madurro, A.G. and Madurro, J.M. (2006) *Macromol. Symp*., 245–246, 236–242.
26. Brito-Madurro, A.G., Ferreira, L.F., Vieira, S.N., Ariza, R.G., Goulart, L.R. and Madurro, J.M. (2007) *J. Mater. Sci*., 42 (9), 3238–3243.
27. Ferreira, L.F., Boodts, J.F.C., Brito-Madurro, A.G. and Madurro, J. M. (2008) *Polym. Intern*., 57(4), 644–650.
28. Chen, C.X., Sun, C. and Gao, Y.H. (2008) *Electrochim. Acta*, 53(7), 3021–3028.
29. Karyakin, A.A., Karyakina, E.E. and Schmidt, H.L. (1999) *Electroanalysis,* 11(3), 149–155.
30. Snead, W.K. and Remick, A. E. (1957) *J. Am. Chem. Soc*., 79(23), 6121–6127.
31. Menezes, H. A. and Maia, G. (2006) *J. Electroanal. Chem*., 586(1), 39–48.
32. Hawley, D. and Adams, R.N. (1965) *J. Electroanal. Chem*., 10(5–6), 376–386.
33. Huang, W.S., Humphrey, B.D. and MacDiarmid, A.G. (1986) *J. Chem. Soc., Faraday Trans. I,* 82(8), 2385–2400.
34. Li, Y.F. and Qian, R.Y. (1989) *Synth. Met*., 28(1–2), 127–132.
35. MacDiarmid, A.G., Chiang, J.C., Richter, A.G. and Epstein, A.J. (1987) *Synth. Met.,* 18(1–3), 285–290.
36. Verma, V.N. and Rai, D.K. (1970) *Appl. Spectrosc*., 24(4), 445–449.
37. Nakanishi K. and Solomon, P.H. Infrared Absorption Spectroscopy, 2nd Ed.; Holden-Day: San Francisco, Chapter 4, 67, 1977.
38. Shan, J.Y., Han, L.Y., Bai, F.L. and Cao, S.K. (2003) *Polym Adv. Technol*.,14(8–12), 330–336.
39. Schröder, K., Meyer-Plath, A., Keller, D. and Ohl, A. (2002) *Plasmas Polym*., 7(2), 103–125.
40. Kang, E.T., Neoh, K.G. and Tan, K.L. (1993) *Surf. Interface Anal*., 20(10), 833–840.
41. Su, Y.Z., Dong, W., Zhang, J.H., Song, J.H., Zhang, Y.H. and Gong, K.C. (2007) *Polymer*, 48(1), 165–173.
42. Liu, S.Y., Cai, Q., Zhu, H. and Jiang, M. (2005) *Chem. J. Chin. Univ*., 26 (6), 1149–1155.
43. Nieto, F.J.R., Andreasen, G., Martins, M.E., Castez, F., Salvarezza, R.C. and Arvia, A.J. (2003) *J. Phys. Chem. B*, 107(41), 11452–11466.
44. Fusalba, F. and Belanger, D. (1999) *J. Phys. Chem. B*, 103 (42), 9044–9054.
45. Bonné, M.J., Helton, M., Edler, K. and Marken, F. (2007) *Electrochem. Commun*., 9(1), 42–48.